Random-walk simulations of NMR dephasing effects due to uniform magnetic-field gradients in a pore

R. M. E. Valckenborg,* H. P. Huinink, J. J. v. d. Sande, and K. Kopinga
Department of Applied Physics, Eindhoven University of Technology, P.O. Box 513, 5600 MB Eindhoven, The Netherlands
(Received 1 July 2001; published 24 January 2002)

A random-walk simulation program was developed to study the effect of dephasing spins in a uniform magnetic-field gradient in a porous material. It is shown that this simulation program correctly reproduces basic nuclear magnetic resonance behavior, such as the formation of a spin echo. The spin-echo decay due to dephasing in a nonrestricted medium gives the well-known exponential relation containing the cube of time, whereas the spin-echo decay due to dephasing in a porous material gives a monoexponential decay. By varying the pore size and magnetic-field gradient, the motional averaging regime and the localization regime can be simulated. Moreover, the unknown intermediate regime is investigated. By choosing the right scaling parameters, the spin-echo decay due to dephasing in a pore can be described by one master curve for all pore sizes and gradient strengths. This master curve reveals a small intermediate regime, perfectly symmetrical around the gradient for which the dephasing length is exactly equal to the structural length of the pore.

DOI: 10.1103/PhysRevE.65.021306 PACS number(s): 81.05.Rm, 05.40.Fb, 76.60.−k, 78.55.Mb

I. INTRODUCTION

The field of nuclear magnetic resonance (NMR) in porous materials is very broad. All kinds of porous materials have already been studied with NMR. The most popular class of materials are biological tissues. Also rocks [1] and building materials such as concrete [2] and wood are imaged by a lot of groups. One of the main research topics of our group is the moisture transport through porous building materials. A building material, difficult to investigate with NMR, is fired-clay brick [3]. Because of the high iron content in this material, the internal magnetic field is very inhomogeneous and the inhomogeneities are relatively large compared to, for example, biological tissues. We have measured the resulting internal magnetic-field gradients in both the base product clay [4] and in the end product fired-clay brick [5]. The major consequence of those high internal gradients is the large enhancement of the dephasing of the spins. Therefore, the transverse magnetization decays much faster in those type of materials than in materials with a comparable pore size but without magnetic impurities.

The importance of diffusion for the dephasing behavior of the magnetic spin moments was already realized by Hahn in his classical paper on spin echoes [6]. He left it as an exercise to the reader to see that dephasing in a constant magnetic-field gradient will lead to an exponential decay, cubic in time. A few years later, Carr and Purcell [7] gave the solution using random walks. They also proposed a pulse sequence that compensates largely for dephasing due to diffusion; it is called the Carr-Purcell-Meiboom-Gill pulse sequence. In 1956, Torrey extended the Bloch equation with the diffusion term, giving the Bloch-Torrey equation [8]. Douglass and McCall [9] solved this equation and found the same solution as Hahn for the free-diffusion situation.

The first measurements of dephasing in a restricted geometry were done by Wayne and Cotts [10] in 1966. In the subsequent paper, Robertson [11] provided the theoretical framework to explain the experimental results. One decade later, Neuman [12] derived the same results for a restricted geometry by a different method, which shows resemblance with the random-walk method.

Recently, Swiet and Sen [13] reconsidered the Bloch-Torrey equation and found two asymptotic situations. The assumption of small phase accumulations (e.g., dephasing of water in a silica gel) leads to the results of Douglass and McCall, and Neumann. The assumption of large phase accumulations (e.g., dephasing of water in a building material) gives a solution for both the free-diffusion and the restricted-diffusion situation. Hürlimann [14] gave an overview of all the different regimes that can be attributed to dephasing in a constant magnetic-field gradient, depending on diffusion time, pore size, and gradient strength. Although the equations describing the asymptotic situation are clear, and also the solutions for these limiting situations are known, there exists an intermediate regime with an unknown magnetization decay. In order to get a better understanding of all these regimes, including the intermediate regime, we developed a simple random-walk simulation model accounting for phase accumulation.

In Sec. II, the NMR dephasing theory will be presented including the asymptotic solutions of the Bloch-Torrey equation. In Sec. III, the simulation method is explained. Section IV A contains the numerical details of the simulation. The model is checked by simulating the free-diffusion situation in Sec. IV B. More interesting are the simulations of restricted diffusion. The model system consists of a spherical pore with a homogeneous magnetic-field gradient, where pore size and magnetic-field gradient strength are varied. The spin-echo decay in the various asymptotic regimes will be simulated and compared to the analytically derived results. Our major question: How the spin-echo decays in the intermediate regime will be addressed in Sec. IV C. The last Sec. V contains the conclusion and discussion.

*FAX: ++31 40 2432598.
Email address: R.M.E.Valckenborg@tue.nl

II. NMR

The simulation program is written to get a better understanding of the dephasing and rephasing behavior of an ensemble of transverse magnetic moments. Therefore, the longitudinal component will not be considered. The transverse magnetic moment is subject to an exponential decay with time constant T_2. The total frequency of events leading to decay ($1/T_2$) is the sum of relaxation events ($1/T_{2,\mathrm{relax}}$) and dephasing events ($1/T_{2,\mathrm{dephase}}$), when no correlation between these effects exists. Although this is subject of current research [5], it is common practice to split the total transverse decay in a relaxation part and a dephasing part. In this paper we only consider the dephasing part.

First, the magnitude of the Hahn spin echo will be given for an infinite system in which the particles and hence the spins can diffuse freely. The magnetic-field variation is limited to the situation of a constant magnetic-field gradient g. The transverse magnetic moment M is described by [6]

$$M(t_E)=M_0\exp\{-\tfrac{1}{12}(\gamma g)^2 D\, t_E^3\}, \tag{1}$$

where M_0 is the equilibrium magnetization, t_E is the spin-echo time, which is equal to exactly two times the interpulse time, D is the self-diffusion coefficient, and γ is the gyromagnetic ratio ($\gamma=2.67\times10^8$ rad/Ts for ^{1}H). If the particles are restricted by a porous material, they cannot diffuse freely anymore. Therefore, the dephasing part of the spin echo will deviate from the above result. To describe the dephasing behavior for the restricted-diffusion situation, three length scales have to be compared. The first is the diffusion length

$$l_D=\sqrt{6Dt_E}, \tag{2}$$

which is the mean distance a particle can travel during time t_E if it is not hindered. The second length scale is the pore size or structural length l_S, which can also be written as the volume of the pore divided by the surface area of the pore V/S. For example, a spherical pore has a structural length that is equal to one-third of the radius of the pore. The third length scale is the dephasing length

$$l_g=\left(\frac{D}{\gamma g}\right)^{1/3}, \tag{3}$$

which is the distance a particle must travel, to dephase by one full cycle (2π) in the magnetic-field gradient.

If the structural length l_S is shorter than the dephasing length l_g and the diffusion length l_D, the magnetization decay is in the so-called motional averaging regime. In that case, the particles probe all parts of the pore. They average their local magnetic field by their diffusive motion. The magnetization of water between two parallel reflecting plates decays according to [11]

$$M(t_E)=M_0\exp\left\{-\frac{c}{6}\frac{(\gamma g)^2 l_S^4}{D}t_E\right\}$$
$$=M_0\exp\left\{-\frac{c}{6}\left(\frac{l_D}{l_g}\right)^2\left(\frac{l_S}{l_g}\right)^4\right\}, \tag{4}$$

where l_S is the plate distance. This has been confirmed by experiments [10]. The above result will hold for all kinds of pore geometries but with a different numerical prefactor [12]. Our main interest is the spherical pore, in which case the geometrical factor $c=\frac{8}{175}$ [12].

If the dephasing length l_g is shorter than the structural length l_S and the diffusion length l_D, the magnetization decay is in the so-called localization regime This happens if the magnetic-field gradient is very strong and the particle has already dephased significantly, before it can hit a pore wall. Swiet and Sen [13] have shown for spins restricted between two parallel plates

$$M(t_E)=M_0\, c\,\frac{l_g}{l_S}\exp\left\{-\frac{a_1}{12}(\gamma g)^{2/3}D^{1/3}t_E\right\}$$
$$=M_0\, c\,\frac{l_g}{l_S}\exp\left\{-\frac{a_1}{12}\left(\frac{l_D}{l_g}\right)^2\right\}, \tag{5}$$

where $a_1=1.02\ldots$ is the first zero of the derivative of the Airy function and $c=5.88\ldots$. The prefactor reflects the fraction of the spins that are contributing to the signal. Also for this regime other geometries will give other numerical prefactors. Hürlimann [15] gave it the name ''localization regime,'' because the magnetization is not homogeneous in the pore. In parts of the pore with a strong magnetic-field gradient, the decay will be fast. An accumulation of magnetization will occur at places where the magnetization decay is small. These are regions with a relatively low magnetic-field gradient or regions with restricted diffusion in the neighborhood of the pore wall. Hence, in the case of a uniform magnetic-field gradient, only the restriction of the pore wall gives low magnetization decay. This effect is also observed in NMR imaging experiments and called ''edge enhancement'' [16].

III. SIMULATION METHOD

A. Model system

We consider a porous sample with an arbitrary geometry in the directions perpendicular to the magnetic-field gradient and with a finite size L in the z direction parallel to the magnetic-field gradient. We assume that this porous sample consists of N randomly distributed identical pores with a volume V and a surface area S. The pores are not connected, but are all isolated. Below, it will be shown that in this system only the dephasing effect of one single pore is needed in the simulations. Of course only the ^{1}H nuclei of the water molecules in the completely water-saturated pores are considered. We assume that one pore contains K spin moments moving via Brownian motion. We neglect magnetic susceptibility differences between the water filled pore space and the pore matrix material. Therefore, also inside the pore, the

magnetic-field gradient is taken perfectly constant. It has been shown [7] that only the z component of this magnetic field is important when the magnitude of the magnetic-field variations is much smaller than the main magnetic field. Therefore in the simulations, the other magnetic-field components will not be considered.

B. Free induction decay

The spins start with maximum transverse magnetization and zero phase at the beginning of the simulation. This means that at $t=0$, the 90° pulse just flipped the spin moment of all particles into the transverse plane. The magnitude and the phase of the magnetization M, which can be measured in an experiment by sampling the free induction decay (FID), is the ensemble averaged spin moment of all particles

$$M = M_0 \langle \exp(i\varphi) \rangle \equiv \frac{1}{N} \frac{1}{K} \sum_{n=1}^{N} \sum_{k=1}^{K} \exp(i\varphi_n^k), \tag{6}$$

where the superscript k runs over all particles K and the subscript n runs over all pores N. If the phase φ_n^k of all particles is known, also the resulting magnetization is known and can be compared with experimental data. The Larmor frequency of each particle is equal to the magnetic field times the gyromagnetic ratio γ. Hence the phase of each particle is equal to the time integral of this product

$$\varphi_n^k = \gamma \int_0^t B(z_n^k(\tau)) d\tau, \tag{7}$$

where $B(z_n^k)$ is the magnetic field at the position z_n^k of particle k inside pore n, that can be written as

$$B(z_n^k(t)) = B_0 + g z_n^k(t), \tag{8}$$

where B_0 is the main magnetic field and g is the constant magnetic-field gradient strength. Because all pores are identical, the possible positions of a spin with respect to the center of the pore are identical in all pores. Therefore, the magnetic field can be split into three contributions

$$B(z_n^k(t)) = B_0 + g z_{n0} + g \tilde{z}^k(t), \tag{9}$$

where $\tilde{z}^k$ is the position of spin k with respect to the center z_{n0} of pore n. Substitution of this expression into Eq. (6) gives the following product:

$$M = M_0 \exp(i\gamma B_0 t) \frac{1}{N} \sum_{n=1}^{N} \exp(i\gamma g z_{n0} t) \times \frac{1}{K} \sum_{k=1}^{K} \exp\left[i\gamma g \int_0^t \tilde{z}^k(\tau) d\tau \right]. \tag{10}$$

The first term at the right-hand side of Eq. (10) gives the contribution of the main magnetic field to the total phase. In a normal FID or spin-echo experiment the NMR signal is demodulated with the Larmor frequency corresponding to B_0, and hence there will be no phase accumulation from this contribution.

The second term at the r.h.s. of Eq. (10) can be solved analytically. To this end a spatial pore distribution function $P(z)$ is introduced, which is normalized as follows:

$$\int_{-L/2}^{L/2} P(z) dz = N. \tag{11}$$

With this function, the summation over all pores can be rewritten to an integral

$$\int_{-L/2}^{L/2} P(z) \exp(i\gamma g z t) dz. \tag{12}$$

This integral can be solved for a given distribution of pores within the sample. A uniform pore distribution $P(z)=N/L$ gives the following in the absence of diffusion:

$$M = \frac{2N}{\gamma g L t} \sin\left(\frac{1}{2} \gamma g L t \right), \tag{13}$$

which is the well-known sinc function, describing the envelope of the FID of a homogeneous, finite sample in the presence of a constant magnetic-field gradient.

The third term at the r.h.s. of Eq. (10) gives the contribution of the diffusing particles in the local field of one pore. This term cannot be simplified analytically, because it contains the time integral over the phase accumulation during a random walk. Therefore a simulation is needed to evaluate this term for all random paths of all particles. In the simulation model, these random walks are generated for various pore sizes and gradient strengths g, which influence the accumulated phase. The fastest way to simulate a random motion is by a discrete hopping of particles. This implies that the time integral is divided into J discrete time steps $\Delta\tau$ ($t = J\Delta\tau$), in which the particles can jump randomly from one position to another

$$\int_0^t \tilde{z}^k(\tau) d\tau = \Delta\tau \sum_{j=1}^{J} \tilde{z}_j^k. \tag{14}$$

C. Spin echo

In a spin-echo experiment, a 180° pulse is applied to the system at a certain time $t=J\Delta\tau$ and the signal at time $2t$ is called the spin echo. The phase evolution after the 180° pulse is often referred to as rephasing. For stationary spins one can imagine that the accumulated phase is inverted and accumulates again to exactly zero at the spin-echo time. For diffusion processes, this rephasing is not complete, because the spins do not follow the same trajectory as before the 180° pulse.

The magnetization of a spin echo can be calculated in the same way as for the FID [Eq. (10)]. Again the contribution of the main magnetic field is zero. The contribution of the dephasing effect of all the different pores can be calculated analytically. For a constant magnetic-field gradient this con-

tribution is zero. This is not surprising, because it is commonly known that a 180° pulse refocuses all dephasing effects due to static magnetic field inhomogeneities. However, the dephasing described by the third term at the r.h.s. of Eq. (10) is not canceled by the 180° pulse, but gives the extra attenuation of the spin echo due to diffusion effects. The phase of the particles in the pore can be written as

$$\varphi_n^k = \gamma g \left[\int_t^{2t} \tilde{z}^k(\tau) d\tau - \int_0^t \tilde{z}^k(\tau) d\tau \right]. \tag{15}$$

Also this time integral of the diffusion process is converted to a series of discrete hopping steps

$$\varphi_n^k = \gamma g \Delta\tau \left[\sum_{j=J+1}^{2J} \tilde{z}_j^k - \sum_{j=1}^{J} \tilde{z}_j^k \right]. \tag{16}$$

Now only the path of the randomly moving spins has to be simulated to obtain the magnetization of the spin echo.

D. Random walk

For computational reasons, we have chosen to generate random walks on a discrete lattice. On a lattice, a particle only has to be moved randomly from one node to another, which can be done numerically with some very fast bit shifts. Continuous random walks, on the other hand, use randomly chosen radii and angles, which require inefficient cosine and sine instructions.

The mean squared displacement $\langle R^2 \rangle$ of Brownian motion is given by

$$\langle R^2 \rangle = 2d\,D\,t, \tag{17}$$

where t is the diffusion time, D is the self-diffusion coefficient, and d is the number of dimensions.

The mean squared displacement $\langle R^2 \rangle$ of a random walk on a simple cubic lattice is given by

$$\langle R^2 \rangle = n\,l^2, \tag{18}$$

where n is the number of simulation steps, and l is the distance between two neighboring lattice points or the distance of a random step when simulating without a lattice. So in three dimensions, during a simulation time step $\Delta\tau$ a particle can move to one of its six neighboring lattice points at distance l. To simulate Brownian motion, Eq. (17) has to be equal to Eq. (18). The diffusion time t is equal to the product of the time of one simulation step $\Delta\tau$ and the total number of simulation steps n. In the simulation, the time step, therefore, has the following value:

$$\Delta\tau = \frac{l^2}{2d\,D}. \tag{19}$$

IV. RESULTS

First, some numerical aspects will be considered. Next, the simulation model is checked with the case of free diffusion. Finally, the simulation is used to calculate the spin-echo decay in a restricted geometry. The asymptotic solutions of the motional averaging and the localization regime are calculated and presented in one master curve. This figure can give an answer to the question: How is the dephasing in the intermediate regime?

A. Numerical aspects

Because of our main interest in moisture transport in porous building materials, we take water as fluid, for which $D = 2.5 \times 10^{-9}$ m^2/s. Of course our lattice is finite. We can simulate all three dimensions with a typical lattice size varying between 100 nm and 100 μm, cubic. For simulation reasons, one would describe a free-diffusion situation with periodic boundary conditions. This means that a particle that leaves the lattice through a certain boundary, will enter the lattice through the opposite boundary. However, in our simulation this is not possible, because the dephasing at, for instance, the left boundary can be very distinct from the dephasing at the right boundary. Therefore, we have put perfectly absorbing walls at the boundary of our lattice. So, if a particle hits this wall it will be removed from the simulation.

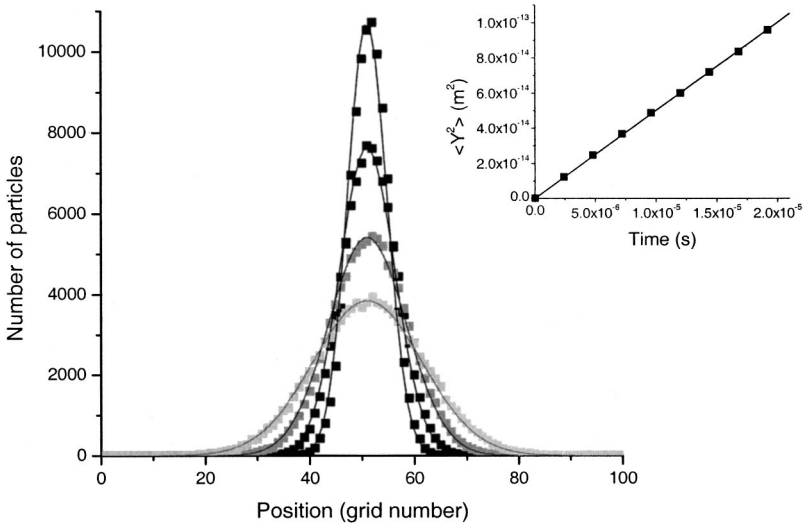

FIG. 1. Y component of the simulated particle distribution at various times t. Solid squares are points from the simulation. The solid curves are the result of fitting a Gaussian function to the data. At $t = 0$, all particles are in the middle of the lattice. The inset shows the mean squared displacement of the particles as a function of time.

For the simulations of free diffusion, in the beginning all particles are put in the middle of the lattice and it is checked that at the echo time only a small fraction of the particles is removed by this mechanism to be sure that it has only a minor influence on the results. For the simulations of a spherical pore, there is no problem because the particles can never reach the lattice boundary. The pore wall perfectly reflects the particles.

The typical number of lattice points is $100\times100\times100$. So l varies between 1 nm and 1 μm, giving a simulation time step $\Delta\tau$ varying between 10^{-10} s and 10^{-4} s. The smallest echo time that can be measured experimentally by our NMR scanners is about 100 μs [17]. This time is reached in the simulations very quickly (for the worst case situation of a cubic 100 nm lattice, in 10^6 diffusion steps). The longest time we consider in our simulations is 10 s, because at that time the normal bulk relaxation time of water will have decayed the spin-echo intensity to a level below the noise, preventing further study of the dephasing behavior. This may result in a very time consuming simulation (for the worst case situation up till 10^{11} diffusion steps). The number of particles is typically $K=10\,000$, which appears to give a signal-to-noise ratio of $S/N=100$. For some simulations, the noise level had to be decreased, in which case $K=10^6$ was taken.

B. Free diffusion

The particles should perform a Brownian random walk when they are allowed to move freely in the lattice space. To demonstrate this, all particles are put in the middle of the lattice at $t=0$. This is allowed, since there is no interaction between the particles themselves. The total lattice length is set to 3 μm.

The y component of the spatial distribution of the freely moving spins at certain times is shown in Fig. 1. The curves are fits of a Gaussian function through the data points at various times. As can be seen, the particles spread Gaussian, as expected. In the inset of Fig. 1, the mean squared displacement in the y direction is shown as a function of time. The simulated results were found to agree with the mean squared displacement given by Eq. (18). Therefore it can be concluded that the particles in the lattice space of the simulation behave Brownian. This check was also performed for the x and z components.

The summation of all spins has to give a FID after the 90° pulse. Also a spin echo has to appear at t_E. Both effects are demonstrated in Fig. 2. At $t=0$ the 90° pulse is given and at $t=5$ ms the 180° pulse is given. The spin echo appears nicely at $t_E=10$ ms. To obtain this picture, also the second term at the r.h.s. of Eq. (10) was taken into account, because this causes the modulation of both the FID and the spin echo [cf. Eq. (13)]. The dotted line shows the dephasing due to diffusion predicted from theory that is only valid at spin-echo time t_E. If we define the magnetization at t_E as the spin-echo intensity, as usual, this intensity can be evaluated as a function of spin-echo time for all kinds of geometries and magnetic fields.

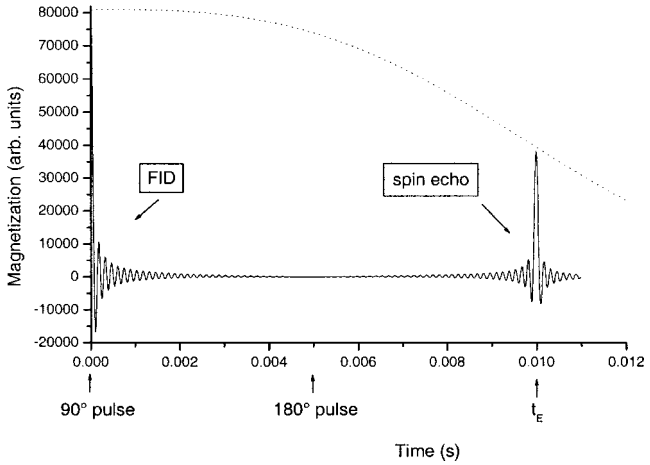

FIG. 2. The solid lines show the simulated transverse magnetization during a spin-echo experiment in the case of free diffusion. The 90° and 180° pulses are given at $t=0$ and at $t=5$ ms, respectively. The dotted line shows the dephasing due to free diffusion.

There is no bulk relaxation mechanism in this simulation and there are no walls in the case of free diffusion. Hence, the spins cannot relax by those mechanisms, but they do dephase. As already mentioned in Sec. II, the spin-echo decay due to dephasing can be described by Eq. (1).

Figure 3 shows the spin-echo intensity as a function of time for a gradient of 10 T/m. The solid curve in this graph is a fit to Eq. (1), which gives a gradient of (9.8 ± 0.1) T/m. The small deviation from the gradient strength used in the simulation is caused by the absorbing walls at the boundary of the lattice. As mentioned above, particles that diffuse out of the lattice space are removed from the simulation, whereas in a real experiment particles that diffuse out of the NMR sensitive region can diffuse back after a while and contribute to the signal.

C. Restricted diffusion

The spins will dephase slower in a restricted geometry than in the case of free diffusion. For restricted diffusion, the

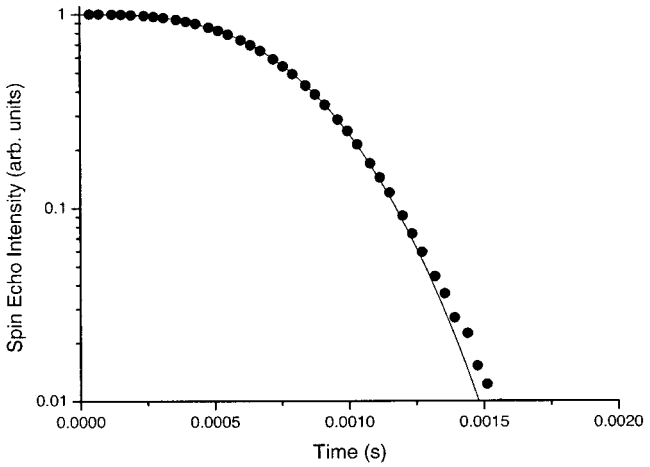

FIG. 3. The spin-echo intensity as a function of time for a constant magnetic-field gradient of 10 T/m. The solid circles are simulated spin-echo intensities, the line is a fit of the free-diffusion equation.

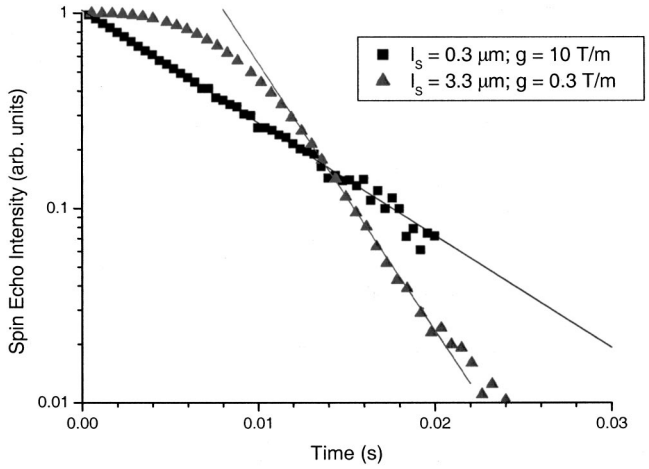

FIG. 4. The spin-echo intensity as a function of time for a pore size of $l_S=0.3$ μm and a uniform gradient $g=10$ T/m; and for a pore size of $l_S=3.3$ μm and a uniform gradient of $g=0.3$ T/m.

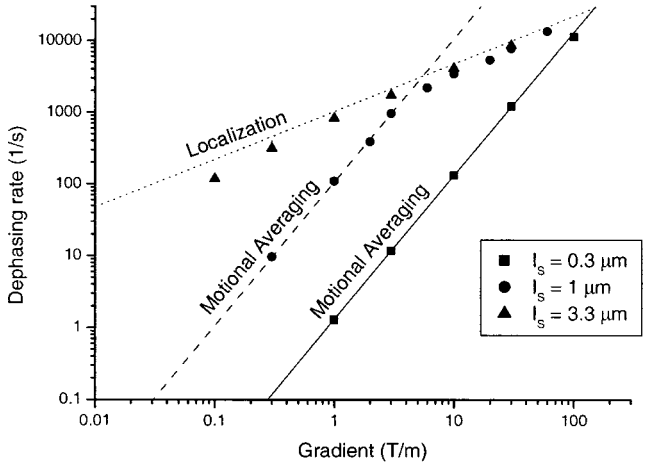

FIG. 5. The simulated spin-echo decay rate due to dephasing for various pore sizes as a function of the gradient field. The solid and dashed lines with slope 2 are the analytical solutions for the motional averaging regime. The dotted line with slope 2/3 shows the $g^{2/3}$ behavior for the localization regime.

diffusion length has to be larger than either the structural length or the dephasing length. As discussed in Sec. II, there can be two different situations. If the dephasing length is smaller than the structural length, the particles are in the localization regime. If the dephasing length is larger than the structural length, the particles are in the motional averaging regime. The spin-echo decay in both regimes is monoexponential, but with a different decay rate [Eq. (4) and (5)].

In Fig. 4 two examples of simulations of the spin-echo decay in a restricted geometry are given. The first corresponds to a pore size of 0.3 μm and a gradient strength of 10 T/m. The transition from free-diffusion behavior to restricted-diffusion behavior will occur when the diffusion length becomes of the order of the pore size. The diffusion length is 0.3 μm, at $t=44$ μs, for Brownian motion [cf. Eq. (17)], i.e., before the first spin echo is created. Therefore all the spin echoes in this experiment will correspond to the restricted-diffusion regime. This is in agreement with the data in Fig. 4, because no transition can be seen and a perfect monoexponential decay is observed. When a larger pore is simulated, this transition from free diffusion to restricted diffusion becomes visible. For example, the second simulation reflects a pore size of 3.3 μm and a gradient strength of 0.3 T/m. In that case the diffusion length equals the pore size at $t=4.4$ ms, which is in agreement with the observation in Fig. 4. The decay in the restricted-diffusion regime after this transition time is monoexponential. A fit of such a decay to the data is shown in the figure by a straight line.

The spin-echo decay has been simulated not only for these two examples, but for various gradient strengths (hence giving various dephasing lengths) and for various pore sizes. In Fig. 5 the decay rate (resulting from a monoexponential fit to the data after the transition time) is plotted as a function of gradient strength. The two straight lines with slope 2 reflect predictions for the motional averaging regime [cf. Eq. (4)]. The slope of the fit to the simulation results for the 0.3 μm pore (1.98 ± 0.02) is in perfect agreement with the theory [cf. Eq. (4)]. One should note, that also the geometrical factor as calculated by Neuman [12] for a spherical pore, yielding a factor of 1.31 $s^{-1}(T/m)^{-2}$, agrees nicely with the simulation results (1.34 ± 0.07) $s^{-1}(T/m)^{-2}$. The dotted straight line with slope 2/3 is a guide to the eye for the localization regime [cf. Eq. (5)]. For this regime the exact solution for a spherical pore is unknown. The exact solution for spins confined between two parallel plates [13] has a numerical prefactor in the exponent of 1.02 [cf. Eq. (5)], whereas we find for our spherical pores a prefactor of 1.6.

Reconsider the theory of the two asymptotic regimes. For a pore size $l_S=0.3$ μm, the dephasing length is equal to l_S at a gradient of 252 T/m [Eq. (3)]. For all gradient strengths smaller than this value, the dephasing length is larger than the structural length. Therefore the motional averaging regime should be applicable for all gradients smaller than about 250 T/m. This is in agreement with the observation in Fig. 5 that all simulated gradient strengths correspond to the motional averaging regime. For a pore size $l_S=1$ μm, the dephasing length is also 1 μm, at a gradient of 9.3 T/m. Therefore a transition from the motional averaging regime into the localization regime is expected around this gradient strength. In Fig. 5 it can be seen, that this transition indeed occurs at about 10 T/m. For pore size $l_S=3.3$ μm, the dephasing length is also 3.3 μm, at a gradient of 0.3 T/m. Therefore, the spin-echo decay should be described by the localization regime for all used gradient strengths, except the simulations for which $g=0.1$ T/m and perhaps $g=0.3$ T/m as is indeed shown by the corresponding data in Fig. 5. In conclusion, the results of the simulations reveal a transition from the motional averaging regime into the localization regime, which is in agreement with the theoretical transition point at $l_S=l_g$. We elucidate this point later on.

Pore sizes smaller than 0.3 μm will be described completely by the motional averaging regime. Simulating these pores becomes time consuming, because the decay rate decreases (which implies a longer simulation time) and also the time step for hopping to another lattice point decreases, as can be seen in Eq. (19) (which implies that more time steps

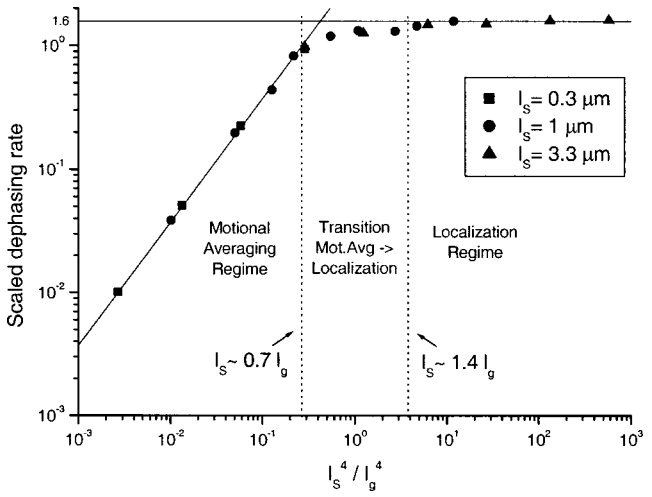

FIG. 6. The scaled decay rate due to dephasing as a function of the scaled parameter $(l_S/l_g)^4$.

are needed for the same simulation time). Pore sizes larger than 3.3 μm will be described completely by the localization regime. For these pore sizes, however, the transition from free diffusion to localization occurs so late in time, that the spin-echo signal has already decayed to a very low level. Simulating these relaxivities is possible but do not give useful results, because in a normal spin-echo experiment the signal-to-noise level will always be on the order of 1000, at best.

The analytical solutions for the motional averaging regime and the localization regime are only asymptotic solutions of the Bloch-Torrey equation. The situation in between these asymptotic situations is called the intermediate regime [14], in which the spin-echo decay is unknown. The results from our simulations show that with increasing gradient strength, the transition from the motional averaging regime into the localization regime is smooth. It is clearly visible in Fig. 5 for $l_S=1$ μm that the spin-echo decay transforms smoothly from the $g^{2/3}$ behavior of the localization regime into the g^2 behavior of the motional averaging regime.

Figure 5 suggests that the decay due to dephasing in the localization regime is identical for all pore sizes. This observation is not surprising because the localization regime is characterized by the fact that the spins are already dephased before reaching the pore wall, given a certain constant gradient. Therefore, the simulated dephasing decay rate can be scaled by dividing it by the theoretical decay rate of the localization regime. The decay rate of the motional averaging regime, on the other hand, depends on both pore size and dephasing length in a known way [cf. Eq. (4)]. Therefore the gradient strength can be scaled by transforming it to the variable $(l_S/l_g)^4$. Figure 6 clearly indicates that the scaled decay due to dephasing as a function of the fourth power of pore size divided by dephasing length gives one master curve for all simulated pore sizes l_S and gradient strengths g, which are incorporated in the dephasing length l_g.

The maximum scaled dephasing rate (horizontal line in Fig. 6) is the dephasing rate corresponding to the localization regime. As mentioned above, we are unable to explain the numerical prefactor of about 1.6 in terms of known theoretical models. The slope of the line of the motional averaging regime is in perfect agreement with the theory, as already mentioned above. With this scaled figure, the transition from the motional averaging regime to the localization regime can be accurately identified. The dashed lines at $l_s=0.7l_g$ and at $l_s=1.4l_g$ define this transition area. It should be noticed that this is exactly around the point $l_S=l_g$, which is commonly assumed in literature [14]. It should also be noticed that the width of the intermediate regime can be understood. Swiet and Sen [13] made the Bloch-Torrey equation dimensionless and showed that the solution of the resulting differential equation is governed by the value of $(l_S/l_g)^3$. This differential equation goes from the one asymptotic solution to the other asymptotic solution if $(l_S/l_g)^3$ varies over one order of magnitude. This means that l_S/l_g only has to vary over a factor of about $\sqrt[3]{10}\approx 2$, which is in agreement with our observation of the width of the intermediate regime.

V. DISCUSSION AND CONCLUSIONS

It is shown that a numerical simulation of the behavior of the spins in a fluid in multiple identical spherical pores nicely reproduces a FID and a spin echo. It is also shown that the simulated random motion of the spins will give Brownian motion with the correct value of the self-diffusion coefficient. The simulated NMR spin-echo decay due to dephasing in a constant magnetic-field gradient for a large enough lattice space gives the well-known free-diffusion spin-echo decay function [Eq. (1)]. The presence of walls in the simulation lattice space transforms this free-diffusion result into the restricted-diffusion result, which is known to be monoexponential. All these results confirm that our simulation model is correctly reproducing real NMR behavior and therefore suitable to investigate unknown situations.

For a pore with a typical pore size of 0.3 μm, the dephasing is described by the motional averaging regime. For a pore with a typical pore size of 3.3 μm, the dephasing is described by the localization regime. Both asymptotic situations were already predicted in the literature [14]. However, the intermediate situation was unknown. The simulations presented in this paper describe this intermediate regime. Moreover, all simulated decay rates due to dephasing can be scaled on one master curve, which gives the complete solution of the problem of a uniform gradient in a spherical pore. From this master curve it is clearly visible that the transition from the motional averaging regime into the localization regime occurs at the gradient strength for which the dephasing length is equal to the pore size $(l_g=l_S)$. It can also be concluded that the transition extends over an intermediate regime for about $0.7<l_S/l_g<1.4$.

In our opinion, the description of clays and fired-clay bricks may require an extension of the model, introduced in this paper. The solid matrix of the porous material has a susceptibility different from the water or air in the pores. This susceptibility mismatch leads to additional magnetic-field gradients [18]. The extent to which the susceptibility mismatch affects the magnetic field inside the bulk matrix or a pore strongly depends on the geometry of the sample [19].

Only ellipsoidally shaped objects will have a uniform magnetic field inside when placed in a homogeneous field. Other geometries lead to nonuniform magnetic fields and, consequently, gradients. Especially sharp corners and wedges will give large local magnetic-field gradients [20]. Therefore, we are currently simulating other pore geometries and more complex magnetic-field distributions, i.e., a summation of dipolar fields that are generated by small iron particles. Preliminary results indicate that the effect of these magnetic impurities may be very important. Because from the present study the intermediate regime in the simple model system with a constant gradient is known, it will be easier to interprete the magnetization decay in more complex situations. The simulation program can also be used to calculate the transverse relaxation in a restricted geometry. In [5], the numerical results of the combined effects of relaxation and dephasing will be presented.

ACKNOWLEDGMENTS

The authors wish to thank L. Pel and M. T. Vlaardingerbroek for stimulating discussions. This project was financially supported by the Dutch Technology Foundation.

[1] G. Borgia, R. Brown, and P. Fantazzini, J. Appl. Phys. **79**, 3656 (1996).
[2] S. Beyea, B. Balcom, T. Bremner, P. Prado, R. A. D. P. Green, and P. Grattan-Bellew, Cem. Concr. Res. **28**, 453 (1998).
[3] L. Pel, K. Kopinga, G. Bertram, and G. Lang, J. Phys. D **28**, 675 (1995).
[4] R. Valckenborg, L. Pel, and K. Kopinga, J. Magn. Reson. **151**, 291 (2001).
[5] R. Valckenborg, Ph.D. thesis, Eindhoven University of Technology, 2001.
[6] E. Hahn, Phys. Rev. **80**, 580 (1950).
[7] H. Carr and E. Purcell, Phys. Rev. **94**, 630 (1954).
[8] H. Torrey, Phys. Rev. **104**, 563 (1956).
[9] D. Douglass and D. McCall, J. Phys. Chem. **62**, 1102 (1958).
[10] R. Wayne and R. Cotts, Phys. Rev. **151**, 264 (1966).
[11] B. Robertson, Phys. Rev. **151**, 273 (1966).
[12] C. Neuman, J. Chem. Phys. **60**, 4508 (1974).
[13] T. D. Swiet and P. Sen, J. Chem. Phys. **100**, 5597 (1994).
[14] M. Hürlimann, J. Magn. Reson. **131**, 232 (1998).
[15] M. Hürlimann, K. Helmer, T. D. Swiet, P. Sen, and C. Sotak, J. Magn. Reson. A **113**, 260 (1995).
[16] P. Callaghan, A. Coy, L. Forde, and C. Rofe, J. Magn. Reson. A **101**, 347 (1993).
[17] K. Kopinga and L. Pel, Rev. Sci. Instrum. **65**, 3673 (1994).
[18] Z. Wang, S. Li, and J. Haselgrove, J. Magn. Reson. **140**, 477 (1999).
[19] M. Vlaardingerbroek and J. D. Boer, *Magnetic Resonance Imaging* (Springer, Heidelberg, Germany, 1996).
[20] R. Brown and P. Fantazzini, Phys. Rev. B **47**, 14 823 (1993).